Open access • Journal Article • DOI:10.1007/S00468-013-0843-7

Structural injury underlying mottling in ponderosa pine needles exposed to ambient ozone concentrations in the San Bernardino Mountains near Los Angeles, California

Pierre Vollenweider, Mark E. Fenn, Terry Menard, Madeleine S. Günthardt-Goerg ...+1 more authors

Published on: 09 Feb 2013 - Trees-structure and Function (Springer Berlin Heidelberg)

Structural injury underlying mottling in ponderosa pine needles exposed to ambient ozone concentrations in the San Bernardino Mountains near Los Angeles, California

Trees (2013) 27:895–911
DOI 10.1007/s00468-013-0843-7

ORIGINAL PAPER

Structural injury underlying mottling in ponderosa pine needles exposed to ambient ozone concentrations in the San Bernardino Mountains near Los Angeles, California

Pierre Vollenweider · Mark E. Fenn · Terry Menard · Madeleine Günthardt-Goerg · Andrzej Bytnerowicz

Received: 3 October 2012 / Revised: 11 December 2012 / Accepted: 8 January 2013 / Published online: 9 February 2013

Abstract For several decades, southern California experienced the worst ozone pollution ever reported. Peak ozone concentrations have, however, declined steadily since 1980. In this study, the structural injuries underlying ozone symptoms in needles of ponderosa pine (*Pinus ponderosa* Dougl. ex Laws.) collected in summer 2006 from one of the most polluted sites in the San Bernardino Mountains were investigated using serial sections examined by light and electron microscopy. Ozone-specific light-green diffuse mottling was observed in the current-year needles, whereas older foliage showed brownish mottling similar to winter fleck injury. Especially, within the outer layers of mesophyll, many markers of oxidative stress, typical for ozone, were observed in both apoplast and symplast. Altogether within cells of mottles, these markers were indicative of hypersensitive-like response, whereas degenerative structural changes were diagnosed in the surrounding mesophyll. Evidence of drought stress and frost injury to older needles was also detected. Hence, mottling injury appeared to be primarily caused by ozone stress, however, other environmental stressors also determined the symptom morphology and distribution, especially within the older foliage.

Keywords Ponderosa pine · Los Angeles basin · Ozone visible injury · Microscopic diagnosis · Needle histochemistry · Mesophyll ultrastructure

Communicated by R. Matyssek.

P. Vollenweider (✉) · T. Menard · M. Günthardt-Goerg
Swiss Federal Research Institute WSL, Birmensdorf, ZH, Switzerland
e-mail: pierre.vollenweider@wsl.ch

M. E. Fenn · A. Bytnerowicz
USDA Forest Service, Pacific Southwest Research Station, Riverside, CA, USA

Introduction

Air pollution levels and the effect on the mountain forests of southern California

For more than 50 years, southern California has experienced some of the highest air pollution ever recorded with ozone (O_3) and nitrogen compounds as the airborne pollutants of greatest concern (Bytnerowicz et al. 2007, 2008; Takemoto et al. 2001). From the 1970s to the present, the June–September 24 h mean O_3 concentration has dropped from 100 ppb with occasional ~600 ppb peaks to 60–70 and ~180 ppb peaks due to the implementation of effective air pollution control measures. However, with AOT40 exposure indices reaching 55–75 ppm h at the most polluted places, southern California still reports the highest ozone levels in the northern hemisphere. The Mediterranean climate and rugged topography—with mountain ranges immediately downwind of the photochemical smog source areas trapping masses of polluted air—contribute significantly to the high amount of air pollution similar to other regions in the world also experiencing elevated levels of O_3 (Dalstein and Vas 2005; de Bauer and Hernandez-Tejeda 2007; Diaz-de-Quijano et al. 2009). Multi-decadal nitrogen (N) deposition caused mainly by elevated concentrations of nitric acid (HNO_3), ammonia (NH_3) and nitrogen oxides (NO_x) have caused N saturation at the most exposed Californian forest sites (Bytnerowicz and Fenn 1996; Fenn et al. 2008). Although not phytotoxic, N antagonistic and synergistic effects with O_3 have had

further detrimental consequences for southern California forests (Grulke et al. 1998; Grulke and Balduman 1999).

Plant damage caused by photochemical smog has been known since the 1950s in southern California and the causal role of ozone, regarding leaf injury, was established experimentally in the 1960s (Miller et al. 1963; Takemoto et al. 2001). Further research has documented: (1) the extent of injury in California forests and the slight reduction following abatement in ozone concentration, (2) alteration of needle physiology with reduction of photosynthetic exchanges and acceleration of needle senescence, (3) alteration in whole-tree biomass and carbon retention in aboveground organs which critically increases tree susceptibility to drought, windthrow and pests, (4) overall negative effects on radial growth and (5) interactions with other stressors such as N deposition, pest outbreak and stand disturbance by forest fires (Grulke et al. 2009; Karnosky et al. 2007; Miller and McBride 1999; Takemoto et al. 2001).

Ozone injury in conifer foliage

Under ozone stress, conifer needles show visible injury in the form of homogeneous (Hartmann et al. 2007) band-like (Flagler and Chappelka 1995; Miller and Evans 1974) needle discoloration or mottling (Sanz and Calatayud 2012; Stolte 1996) which vary in intensity and morphological details depending on the ozone dose and tree species. In pine species, chlorotic mottling is the most frequent injury reported and this symptom is one of the principal parameters used to calculate the Forest Pest Management (FPM) and Ozone Injury Index (OII) in forest health surveys in California and other parts of the US (Arbaugh et al. 1998; Grulke 2003). Morphological traits of mottle characteristics of O_3 stress used for diagnosis versus other biotic (e.g. insect, mite or fungal injury) and abiotic stressors include: (1) diffuse edges, (2) connection to stomata and (3) distribution on the light-exposed side of needles in the sun crown (Günthardt-Goerg and Vollenweider 2007; Miller et al. 1997). Interactions with abiotic stress factors, noteworthy frost in the case of the wintering symptomatic foliage of pines in mountain forests, complicate the diagnosis. Symptoms designated as "winter fleck" have been described and their morphological characteristics do show similarities to O_3-induced mottling (Hartmann et al. 2007; Miller and Evans 1974; Stolte 1996). N compounds and oxidants other than ozone do not induce mottling (Davis 1977; Padgett et al. 2009; Takemoto et al. 2001).

Structural changes to be found in living as well as dead cells form markers of cellular physiological processes and responses (Fink 1999; Günthardt-Goerg and Vollenweider 2007; Jones 2000; Levine et al. 1996) and can be used for the diagnosis of ozone damage (Kivimäenpää et al. 2005; Vollenweider et al. 2003a, b). Several studies have analyzed structural injuries triggered by O_3 stress in conifer needles with (Table 1) or without (Anttonen and Karenlampi 1996; Evans and Leonard 1991; Kainulainen et al. 2000) visible symptoms. In trees showing mottling but generally independent of visible injury, they have documented characteristic changes to the mesophyll structure, whereas other tissues remained nearly asymptomatic. Concerning the microscopic changes underlying mottling, however, little has been published so far. Indeed, these symptoms are difficult to process in view of microscopical analysis because of their (1) poor visibility, further degrading during sample fixation and processing and (2) minute size. Hence, unless special care is taken during sample handling and sectioning, the structural injuries causing mottling are easily missed. Structural injury reported so far for Jeffrey (*Pinus jeffreyi* Grev. & Balf.) or ponderosa pine (*Pinus ponderosa* Dougl. ex Laws.) dates back to the early studies using needle material showing massive visible injury as a consequence of the high doses of ozone which occurred at that time, but which no longer presently exist in California (Table 1).

Study objectives

The aim of this study was to characterize the microscopic changes and the processes leading to mottling injury in pine needles in response to ambient O_3 pollution, as currently occurring in southern California. Needles from ponderosa pine, a pine species with well-documented photosynthetic sensitivity to O_3 (Coyne and Bingham 1982) and showing mottling both in the field (Stolte 1996) as well as in controlled conditions (Richards et al. 1968), were sampled near Camp Paivika (CP), a long-term air pollution/forest health monitoring station in the San Bernardino Mountains near Los Angeles, California, USA (Miller and Rechel 1999). Structural injury underlying mottling was investigated using transmitted light, fluorescence and electron microscopy (EM) and related to specific O_3 or other interacting stress effects (Günthardt-Goerg and Vollenweider 2007; Vollenweider et al. 2003a).

Materials and methods

Study site, climate and air pollution

The CP study site was selected as being one of those consistently displaying the severest ozone injury in the San Bernardino Mountains (Miller and McBride 1999) with OII in 1997, amounting to 57.1 versus 14.6 at an eastern SBM site (authors' unpublished data). It is located directly to the east (ca. 70 km) of Los Angeles at 1,580 m a.s.l. on the

Table 1 Structural injury triggered by O_3 stress in conifer needles showing mottling or other types of necrotic flecks

Species	O_3 treatment/O_3 exposure	Needle sampling	Injury			Reference
			Macroscopic	Histological	Cytological	
P. ponderosa, *jeffreyi*, *coulteri*, *lambertiana*	350 ppb, 9-h day^{-1}, 55 days[a]	Targeted at visible injury	n.i. (chlorotic mottling)	Initial injury in outer layers of mesophyll, with or without association with substomatal areas, progressing inwardly to finally encompass all mesophyll layers	Gradual loss of cell integrity	Evans and Miller (1972a)
P. ponderosa	450 ppb, 12-h day^{-1}, 35 and 8 days[a]	Targeted at visible injury	Chlorotic mottling	Initial injury in outer layers of mesophyll, independent of substomatal areas, progressing inwardly and leading to tissue collapse concomitant to cell death.	Cell death and collapse within 5 days	Evans and Miller (1972b)
Picea abies	n.i.	Targeted at visible injury	Minute necrotic spots	Necrosis and transition area in mesophyll	Necrosis: disrupted cell content, condensation of the cell remnants along cell walls, coarse granular particles in cytoplasm and chloroplasts Transition area: degenerated cytoplasm, coarse granular particles in cytoplasm, chloroplasts with a smaller size and modified shape showing membrane ruptures and stroma degeneration, degenerating mitochondria	Sutinen (1986)
P. abies	50–98 ppb, 7-h day^{-1}, 113–183 days during 3 years[a]	Independent of visible injury	Chlorotic mottling	Initial injury in outer layers of mesophyll facing the sky progressing inwardly and downwardly to mesophyll layers facing the ground	Independent of mottling: decrease in the chloroplast and starch grain size, increased stroma condensation, reduced amount of thylakoid membranes, increased amounts of plastoglobuli, disruption of peroxysomes and mitochondria	Sutinen et al. (1990)
Pinus ellioti	55–71 ppb, 7-h day^{-1}, 17–83 days[a] $\leq$20 ppb[b]	Targeted at visible injury	Chlorotic mottling	Injury in mesophyll	Cell plasmolysis and cytorhisis	Evans and Fitzgerald (1993)
Pinus rigida	50–200 ppb, 8-h day^{-1}, 13 weeks[a]	Independent of visible injury	Chlorotic needle tips, curvature at mid-needle	Injury starting in outer layers of mesophyll, around the substomatal cavities and progressing towards inner mesophyll and vascular bundle, accumulation of intercellular debris in mesophyll, degeneration of endodermis and phloem collapse	Condensation of the chloroplast stroma, thylakoid swelling, increased plastoglobuli density	McQuattie and Schier (1993)

Table 1 continued

Species	O_3 treatment/O_3 exposure	Needle sampling	Injury			Reference
			Macroscopic	Histological	Cytological	
Pinus halepensis	150–600 ppb, 7–12-h day^{-1}, 2–16 days[a]	Independent of visible injury	Light-yellowish flecks on $\geq$50 % of the needle	Injury primarily in outer layers of mesophyll and around the substomatal cavities	Protoplasm disruption, decrease in the chloroplast and starch grain size, increased stroma condensation, thylakoid swelling and membrane disruption, increased fatty acid saturation	Anttonen et al. (1995)
Pinus sylvestris	100–600 ppb/ 12–8.4 ppm h, 2–28 days[a]	Independent of visible injury	With higher O_3 exposure only, development of large necrotic flecks in $\geq$50 % of foliage	Most severe injury in outer layers of mesophyll and around the substomatal cavities	Mesophyll cell collapse at high O_3 concentration, decrease in the chloroplast and starch grain size, increased stroma condensation and granulation, increase in the plastoglobuli density at low and decrease at high O_3 concentration	Holopainen et al. (1996)
Pinus taeda	47–98 ppb, 12-h day^{-1}, 140 days[a]	Independent of visible injury	Chlorotic mottling, water-soaked bands, necrotic spots	n.i.	Alteration of the plasmalemma and chloroplast envelope, decrease in the chloroplast and starch grain size, increased stroma condensation, thylakoid swelling, increase in the density of plastoglobuli	Anttonen et al. (1996)
Abies religiosa	>110 ppb, 4–5-h day^{-1}, 300 days[b]	Independent of visible injury	Whitish stippling apart from the mid-rib coalescing into reddish flecks and developing abaxially prior to needle yellowing and shedding	Discrete necrotic groups of cells with the most severe injury in outer layers of mesophyll	Disrupted cell content, condensation of the cell remnants along cell walls, plasmolysis	Alvarez et al. (1998a)
P. sylvestris	14.5–33 ppm h (AOT40), 20 weeks[a]	Independent of visible injury	Chlorotic mottling and yellowing of the previous needle generation	n.i.	Increased frequency of cytoplasmic ribosomes, transient increase in the condensation of stroma	Utriainen and Holopainen (1998)
P. halepensis	20 ppm h (AOT40)[b]	Including visible injury	Chlorotic mottling	Injury especially in outer layers of mesophyll, around the substomatal cavities and in the vascular bundle	Decrease in the chloroplast size, increased stroma condensation, increased plastoglobuli density, plastoglobuli excretion towards the vacuole, increase in amounts of tannin, starch and lipid	Soda et al. (2000)
Pinus cembra	n.i.	Including visible injury	Photobleaching and mottling	Discrete necrotic groups of cells in mesophyll	Disrupted cell content, condensation of the cell remnants along cell walls, accumulation of proanthocyanidins	Vollenweider et al. (2003a)

Table 1 continued

Species	O_3 treatment/O_3 exposure	Needle sampling	Injury			Reference
			Macroscopic	Histological	Cytological	
P. halepensis	35.4–56.5 ppb/ 15.5–36.7 ppm h (AOT40)[b]	Independent of visible injury	Chlorotic mottling	Injury in mesophyll	In association with mottling: change in the vacuolar tannin structure, decrease in the chloroplast size and frequency, increased plastoglobuli density, increased amounts of peroxysomes and mitochondria, reduced amounts of starch and lipids	Kivimäenpää et al. (2010)

n.i. no indication

[a] Material exposed to O_3-enriched air during fumigation experiments

[b] Material exposed to ambient O_3 levels

crestline within a mixed conifer stand with a western aspect. The climate at CP is temperate to cold, sub-humid and as such, representative of a Mediterranean and mountain area (Walter and Lieth 1967; Fig. 1a). Eighty percent of the annual precipitation is deposited in October–March (Takemoto et al. 2001), mainly in the form of snow and there is a summer drought between mid-April and October. In 2006, with an annual mean temperature of 13 °C and only 717 mm precipitation, CP experienced drier climatic conditions in comparison to averages over the last 50 years, and a more severe summer drought with a precipitation deficit lasting from July to the end of the year (Fig. 1b vs. a).

Bedrock at CP is granitic and soils are coarse-loamy, mixed, mesic, and typical Haploxerolls (Arkley 1981). Forest stands at CP form the western end of the mixed conifer zone in the San Bernardino Mountains. Vegetation type is mixed conifer forest with ponderosa pine and California black oak (*Quercus kelloggi* Newb.) as the most abundant tree species at the site. In 2006, only an open stand remained over a portion of the study plot as a consequence of increased tree mortality following the drought 2002–2004 and a fire in October 2003, which burned a part of the CP site.

Ozone concentrations for the southern California region were obtained from the California Air Resources monitoring network equipped with Thermo Environmental Model 49 UV absorption monitors. Data were presented as the highest 8 h average concentration during the entire year 2006. O_3 concentrations for CP were obtained from the Crestline air monitoring site located 4 km to the east. O_3 exposure indices were calculated using the Ozone Calculator program (William Jackson, USDA Forest Service, http://webcam.srs.fs.fed.us). The SUM00 index is an exposure dose resulting from multiplying all hourly concentrations by time (h). The SUM06 index was derived by multiplying the number of hours when O_3 concentrations were >60 ppb (0.06 ppm) by those concentrations. These two indices were calculated for 24 h for a 4-month period (June 1–September 30). In comparison with the European studies, AOT40 exposure index was also calculated as a cumulative dose of values >40 ppb (0.04 ppm) for the standardized daylight hours (08:00–20:00 PST) during the 6-month growing season (April 1–September 30).

Sampling and microscopic analysis

Sampling occurred on the afternoon of September 10, 2006 and focused on mottling symptoms typical of O_3 stress (Sanz and Calatayud 2012), whilst deliberately excluding material showing other types of injury (Vollenweider and Günthardt-Goerg 2006). One tree displaying representative mottling injury on accessible (1–2.5-m high) branches

exposed to full sunlight was selected. Ten current (C) and ten 1-year-old (C + 1) symptomatic needles were collected along the same branch segments. Older needle generations were not harvested because of the risk of confusion with other stress factors. Symptomatic middle needle segments were trimmed and immediately fixed using 100 % methanol and regular or EM-grade 2.5 % glutaraldehyde—the latter two solutions buffered at pH 7.0 with a 0.067 M Soerensen phosphate buffer—and stored at 4 °C for 12 days. At the Swiss Federal Institute for Forest, Snow and Landscape Research (WSL) laboratory, glutaraldehyde fixed samples were entirely infiltrated with renewed fixing solution by evacuation before storage at 4 °C until further processing. To investigate histological, cytological and histochemical changes in mottling symptoms and surrounding needle parts, samples were processed in three different ways: (1) methanol-fixed samples were hand-microtomed to obtain thick cuttings (30 µm); (2) samples fixed with regular glutaraldehyde were dehydrated with 2-methoxyethanol (three changes), ethanol, n-propanol, and n-butanol (Feder and O'Brien 1968), embedded in Technovit 7100 (Kulzer HistoTechnik) and semi-thin cuttings (2 µm) were sectioned using a Reichert 2050 microtome; (3) EM-grade fixed samples were post-fixed in buffered 2 % OsO_4, dehydrated by a series of graded ethanol, infiltrated by a series of graded propylene oxide/Epon 812 mixture (with DDSA, NMA and DMP hardener), embedded in Epon and ultra-thin cuttings (70 nm) were sectioned using a Reichert UltraCut S ultra microtome. For each type of preparation, batches of serial cross-sections were cut through symptomatic needle segments (about 650 µm of needle tissue per batch) and cuttings at symptom core locations were sorted out. Thick and semi-thin sections were stained with different methods (Table 2), mounted in water or DPX and observed using a Leica microscope Leitz DM/RB, with 5× to 100× objectives and diascopic light illumination. Thin sections were mounted on copper grids and contrasted using saturated uranyl acetate in 50 % ethanol and lead citrate (Reynolds procedure). Sections were observed using a Philips CM 12 transmission electron microscope.

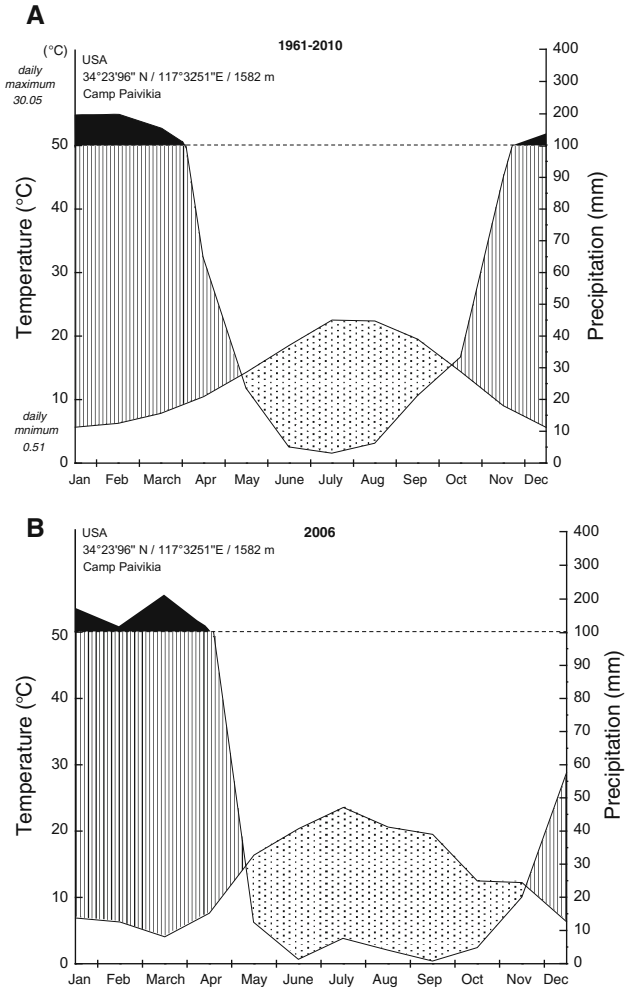

Fig. 1 Climate diagram summarizing the climatic conditions at Camp Paivikia during the 1961–2010 reference period (**a**) and in 2006 (**b**). *Diagrams* are plotted according to Walter and Lieth (1967). Between 0 and 100 mm precipitation monthly, 20 mm on the right ordinate is equal 10 °C of average temperature on the left ordinate. Above 100 mm (*dashed line*), precipitation is plotted using a scale 5 times larger. The dry and moist seasons are outlined with a *dotted line* and *dashed/solid area*, respectively. Mean yearly temperature and precipitation: 13.04 °C and 926 mm between 1961 and 2010 (**a**), 13.03 °C and 717 mm in 2006 (**b**)

Results

Air pollution

In 2006, CP was among the most O_3 polluted sites in southern California with the highest 8 h average concentration of 0.143 ppm (Fig. 2). There were clearly pronounced seasonal differences in O_3 concentrations with low values of the pollutant in the October–March winter season and much higher levels during the summer photochemical smog season (April–September, Fig. 3). Accordingly, average O_3 concentrations in June, July and August were the highest (0.062, 0.059 and 0.061 ppm, respectively). The maximum hourly value of 0.164 ppm at CP was recorded in July, while the mid-winter maximum hourly concentration dropped to 0.050 ppm. The annual average O_3 concentration was 0.042 ppm. The O_3 exposure indices were: SUM00−161.9 ppm h, SUM06−103.3 ppm h, and AOT40−58.34 ppm h. These results confirm the high concentrations of O_3 and its exposure indices at CP. Although the recorded concentrations were lower than in 2002–2005 (figure not shown), they were still higher than other comparable forest sites in North America and Europe (Bytnerowicz et al. 2008).

Visible symptoms in C and C + 1 needles

In C needles from CP, O_3-like visible injury was observed in the form of tiny rounded light green mottles scattered on the unshaded abaxial as well as adaxial needle side exposed to full sunlight. The mottle's average diameter ± SE was 221 ± 20 µm (range 121–305 µm, $n = 10$ symptoms measured using five needles, Fig. 4a, b). These symptoms developed around the stomata amid needle tissue showing a lighter green color than shaded needle parts and they had diffuse boundaries. They were observed on most ponderosa pines at the study site, but were limited to the C needle generation. Contrastingly, in adjacent C + 1 and older needle generations, larger light brownish mottles encompassing several stomatal lines and with sharp boundaries were observed. Their average diameter ± SE was 543 ± 67 µm (range 317–926 µm, $n = 10$ symptoms measured using five needles, Fig. 4c). They were observed on the abaxial and adaxial needle side and their frequency increased with the needle age and full sunlight illumination. Compared to C needles, the C + 1 needles showed a darker green background color.

Needle structure of C and C + 1 needles

In the mesophyll outside of mottles, little vitality differences between cells were observed, but structural gradients were evident (i.e. from the inner to outer mesophyll: an increase in the chloroplast condensation and proanthocyanidin oxidation and an apparent reduction in the chloroplast and starch grain size; figures not shown). Assimilative cells throughout mesophyll were functional as indicated by (1) thin and mostly unlignified cell walls (Figs. 5c, 7d, k), (2) uncondensed cytoplasm with low amounts of lipid droplets (Figs. 5e, 6a, 7g), (3) large and uncondensed nuclei (Figs. 5c, g, 7d, i), (4) chloroplasts with distinct grana, few plastoglobuli and little starch despite sampling in the afternoon (Fig. 6i), (5) peroxysomes and mitochondria without apparent injury and occasional smooth endoplasmic reticulum (Fig. 6a), (6) vacuoles with undisrupted tonoplast and without large lipid accumulation or autophagic remains (figure not shown). However, both inside and outside of mottles, an enlarged periplasm was occasionally observed. In asymptomatic cells, the chloroplasts were small, their stroma generally condensed and the membranes poorly resolved (Fig. 6a, i). Tannins in the form of proanthocyanidins were observed in cell walls, nuclei and vacuoles (Figure not shown). In C + 1 versus C needles, the vacuolar proanthocyanidin deposits had their frequency strongly increased and their shape changed from mostly droplet-like to an homogeneous or finely granular and only occasionally ribbon-like or spongy form (Figs. 7a, d vs. 5a, c, 6a). Other tissues showed a healthy structure and biotic injury was missing.

Structural changes in mottles of C needles

Inside mottles of C needles, the strongest structural changes were found within the outer mesophyll cells adjacent to the substomatal chamber (Figs. 4d, 5b vs. a). Mottles included dead and degenerating cells and the transition to asymptomatic inner or surrounding mesophyll occurred within a single cell layer. At the mottle center, massive cell wall thickening obstructed most of the intercellular space (Figs. 5b, d, h, j, k, 6f). Full embedding in Technovit (Fig. 5)—respectively Epon (Fig. 6)—resin of these cell

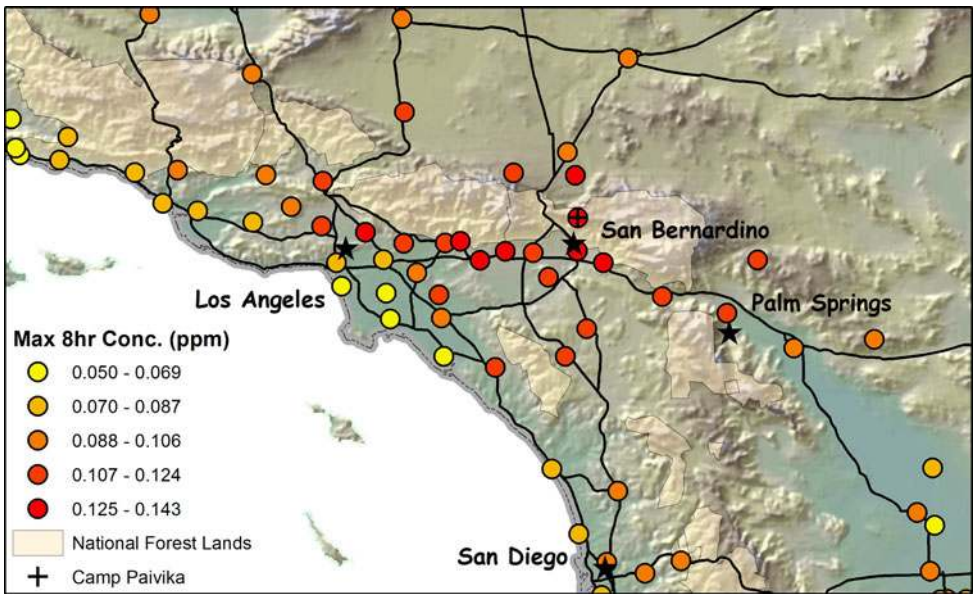

Fig. 2 Maximum 8-h O_3 concentrations throughout southern California in 2006

Table 2 Staining methods (stain dilution in w/v)

Stain	Reference	Solution	Staining time (min)	Color in transmitted light	Excitation (nm)	Histochemical target	Figure
Vanilin acid[a]	Sarkar and Howarth (1976)	Vanilin 10 % in ethanol:HCl 37 % = 2:1	Observed in reagent	Red	–	Proanthocyanidins	Figure not shown
Toluidine blue O[b]	Feder and O'Brien (1968)	0.05 % aq., acetate buffer pH 4.4	10	Blue	–	Metachromatic stain	4d, e, 5a–d, 7a–f, m
Fuchsin acid[b]	Feder and O'Brien (1968)	1 % Fuchsin acid aq.	20	Pink	–	Metachromatic stain	4e, 7a–f, m
Coomassie brilliant blue[b]	Wetzel et al. (1989), modified	0.025 % in 100 % ethanol:acetic acid = 3:1	35	Blue	–	Proteins	5g, h, 7i, j
Calcofluor white Mr2[b]	Munck (1989)	0.1 % in 50 % ethanol aq.	2	–	340–380	Cellulose	Figure not shown
Coriphosphine[b]	Weis et al. (1988)	0.03 % aq.	3	–	450–490	Pectins	7n
PARS[b]	Gahan (1984)	0.5 % periodic acid; Schiff reagent; 0.5 % potassium metabisulfite in 0.05 N HCl	10; 20; 3 × 5	Pink	–	Polysaccharides	5k
Aniline blue[b]	Gerlach (1984)	0.005 % in Soerensen buffer pH 8.2	10	–	340–380	Callose	Figure not shown
Phloro-glucinol[b]	Schneider (1979) as cited by Clark (1981), modified	Saturated in 18 % HCl	Observed in reagent	Pink	–	Lignin	5i, j, 7k, l
Sudan-black B[b]	Brundrett et al. (1991)	0.2 % in 100 % ethanol:glycerin = 1:1	Observed in reagent	Blue-black	–	Lipids	5e, f, 7g, h

Material

[a] Hand-microtome cuttings

[b] Semi-thin Technovit-embedded cuttings

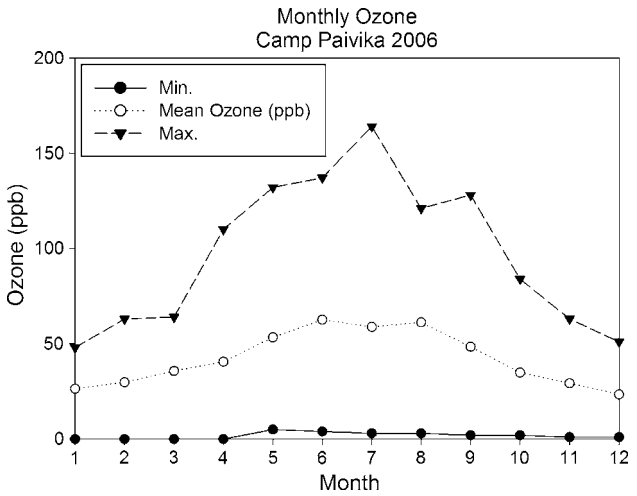

Fig. 3 Seasonal changes (monthly mean, minimum and maximum values) in O_3 concentrations at the Crestline air monitoring station in 2006

wall thickenings and adjacent cells excluded the possibility that these structures resulted from sample processing artifacts. Further, these intercellular masses showed structural traits typical for cell walls, including (1) an ultrastructure similar to middle lamella material (Fig. 6f), (2) a structural continuity with the cell wall outer layers (Figs. 5k, 6f) and (3) a typically polysaccharidic (Fig. 5k) matrix made of mostly pectins. Additionally, small protein (Fig. 5h), lignin (Fig. 5j) and cellulose (figure not shown) fractions were detected, while callose was missing. Heterogeneous and loosely arranged cell debris, structurally and histochemically contrasting with cell wall thickening and presumably leaked from dead cells, were also observed in the intercellular space (Figs. 5b, 6f). Within dead cells, the cell lumen was empty and the condensed cell content remnants were densely packed onto cell walls (Fig. 5d). Surrounding cells showed varying degenerative features indicative of a gradual cell decompartmentation and typically evidenced by blistering of the tonoplast and other membranes (Figs. 5d, 6c). In comparison to the asymptomatic mesophyll, the cell content showed more lipid droplets in the vacuole (Fig. 5f vs. e), but a smaller protein fraction in the cytoplasm (Fig. 5h vs. g). Less vacuolar proanthocyanidins were observed than in the mesophyll outside mottles.

At a subcellular level, the cytoplasm and organelles of cells inside mottles showed advanced degeneration contrasting with the moderate changes found in the surrounding mesophyll (Fig. 6b vs. a). Injury progress in the cytoplasm was evidenced by increasing condensation and formation of coarse granular particles (Fig. 6c–e vs. 6a), lipid accumulation (Fig. 6d), empty vesicle formation (Fig. 6c, d) and tonoplast blistering (Figs. 5d, 6c). In terminal stages, only amorphous and coagulated particles with few still recognizable structures such as large starch grains remained (Fig. 6e). Regarding organelles, nuclei were small, deformed and strongly condensed (picnotic nuclei, Figs. 5d, 6g), mitochondria showed progressive disruption of the matrix and inner membranes and apparently evolved to empty and rather inflated vesicles (Fig. 6c, d, g, h), and

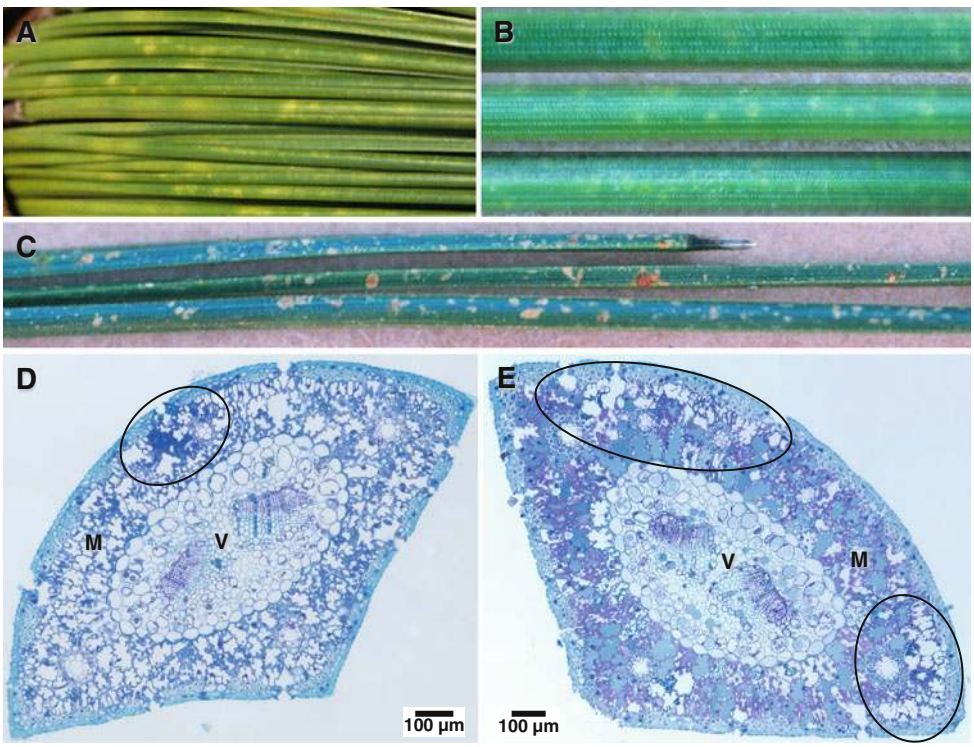

Fig. 4 Macro-(**a**–**c**) and micromorphological (**d**, **e**) characteristics of the mottling symptoms observed at Camp Paivikia in 2006. **a**, **b** *Light-green* diffuse mottling in C needles; symptoms were found on the light exposed side of needles and were centered on stomata. **c**: *Brownish* mottling in C + 1 needles; symptoms were larger than the diffuse symptoms and showed an irregular contour. **d**, **e** Needle serial cross-sections through mottling symptoms. Structural injury (*circle*) was found in outer mesophyll (*M*) cells whereas veins (*V*) showed no injury. In C needles (**d**), injury was restricted to a small group of cells adjacent to stomata. In C + 1 needles (**e**), an extended portion of outer mesophyll was injured

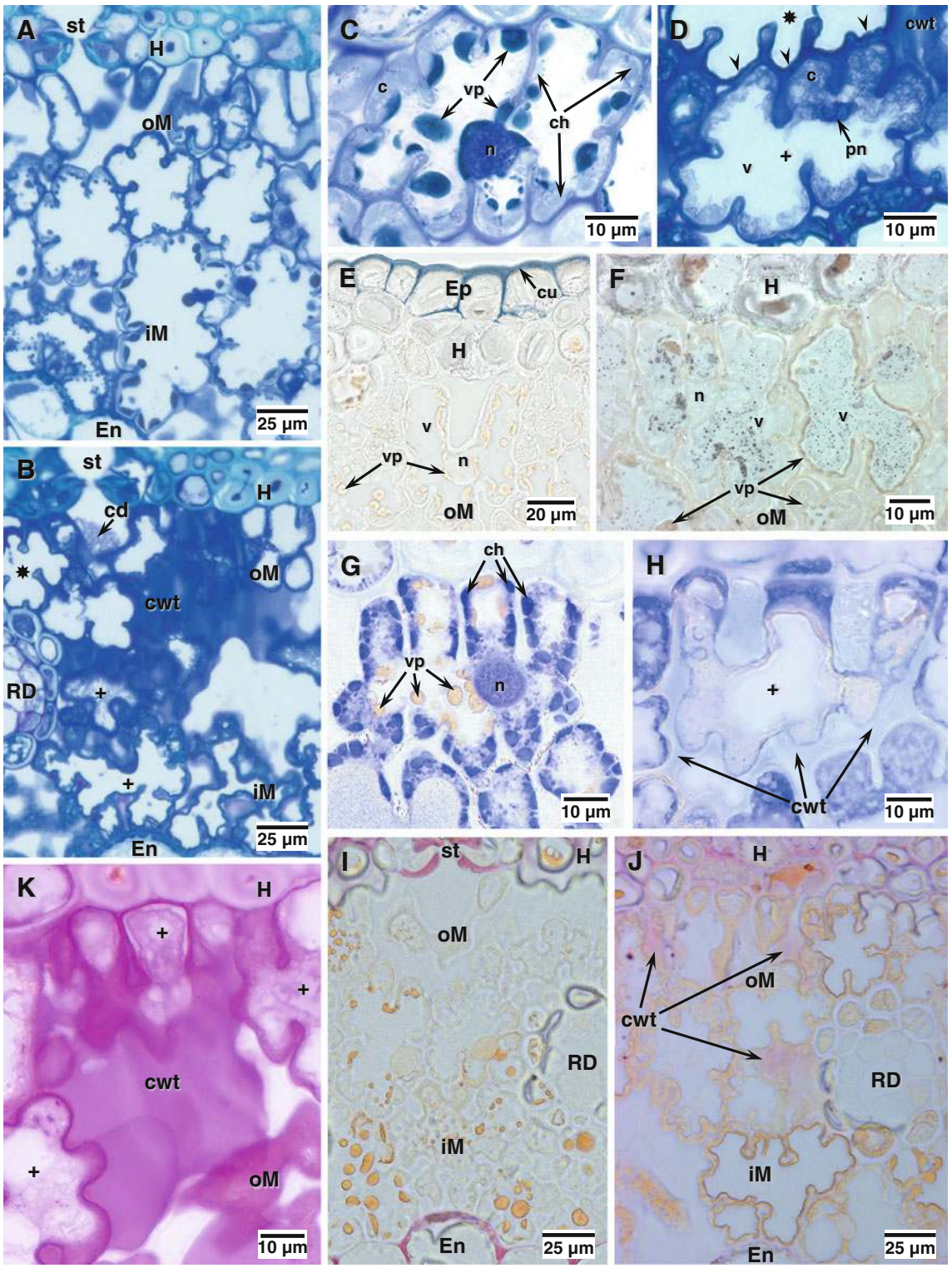

peroxysomes had disappeared. Chloroplasts also showed a characteristic structural evolution including size reduction, a decrease in grana frequency and thickness, an increase in plastoglobuli density and an enhanced stroma condensation (Fig. 6j–l). During the terminal degeneration stages (Fig. 6l), the plastoglobuli were no longer identifiable and the chloroplasts finally disrupted except for the starch grains (Fig. 6e). Degenerative processes in chloroplasts and probably also in other organelles, particularly membrane injury, could contribute to lipid droplet formation

◀ **Fig. 5** Structural (**a**–**d**) and histochemical (**e**–**j**) changes at the tissue (**a**–**b**, **i**–**j**) and cellular (**c**–**h**, **k**) level found inside (**b**, **d**, **f**, **h**, **j**, **k**) versus outside (**a**, **c**, **e**, **g**, **i**) mottling symptoms in mesophyll of C needles showing *greenish* diffuse mottling. **b** (*Mottling*) versus **a** (*no mottling*): Cells within mottled areas were dead (*) or showed advanced degeneration (+). At mottle centre, massive cell wall thickening (*cwt*) filled the whole intercellular space. Other type of intercellular material included amorphous and loosely arranged cell debris (*cd*). **d** (*Mottling*) versus **c** (no mottling): Dead cells showed condensed cell content remnants appressed to cell walls (*arrowheads*), whereas less degenerated cells showed a partly disrupted protoplasm with irregular vacuolar outline and a few still recognizable organelles (*arrows*). Nuclei had shrunken to highly condensed and deformed picnotic structures (*pn*). **f** (*Mottling*) versus **e** (*no mottling*): Lipid droplets (*dark blue*) accumulation in vacuoles of outer mesophyll cells at mottle centers. **h** (*Mottling*) versus **g** (*no mottling*): The protein cell content was decreased, whereas a small protein fraction (light blue staining) was inlayed within the massive cell wall thickenings. **j** (*Mottling*) versus **i** (*no mottling*): Lignin inlay (pink) within the massive cell wall thickenings—notice the constitutively lignified cell walls in hypodermis and endodermis cells. **k** (*Mottling*): The massive cell wall thickenings (*pink*) were primarily made of polysaccharides (pectins). Other structures: *c* cytoplasm, *ch* chloroplasts, *cu* cuticula, *En* endodermis, *Ep* epidermis, *H* hypodermis, *iM/oM* inner/outer mesophyll, *RD* resin duct, *st* stomata, *v* vacuole, *vp* vacuolar proanthocyanidins

(Fig. 6l) prior to accumulation in the cytoplasm (Fig. 6d) and coalescence in the vacuole (Fig. 5f).

Structural changes in mottles of C + 1 needles

Similar to C needles, the most prominent changes in mottles of C + 1 needles were observed in the outer layers of mesophyll, but they extended wider and were not restricted to a single stomatal line (Fig. 4e). Symptoms reached variable depth inside the assimilative tissue, whereas injury to other tissues was generally nonexistent (Figs. 4e, 7b, c vs. a). Cells in rows just below the hypodermis were necrotic and often broken but rarely collapsed and their cell remnants were scattered in the intercellular space (Fig. 7c). In the still remaining complete cells, cell death was indicated by an empty cell lumen presumably as a consequence of tonoplast, plasmalemma and organelle disruption and condensation of oxidized cell content remnants along cell walls (Fig. 7f). A transition zone of cells showing less advanced degenerative features surrounded the necrotic mottle center (Fig. 7b, e). A high level of nuclear material condensation was observed, indicative of chromatin breaking similar to that found after programmed cell death (Fig. 7e; Levine et al. 1996; Alvarez et al. 1998b). Histochemically, the amount of proteins in cells inside mottles was lower than in the asymptomatic mesophyll (Fig. 7j vs. i), whereas the cytoplasmic lipid content was slightly increased (Fig. 7h vs. g). The vacuolar proanthocyanidins inside mottles showed a lower frequency and a ribbon-like structure compared to homogenous filling in the surrounding mesophyll (Fig. 7b, e, vs. a, d). In cell walls, the middle lamella showed a higher degree of lignification than was found in the surrounding mesophyll (Fig. 7l vs. k). In dead cells and in those within the transition to still healthy-looking mesophyll, thickened cell walls, structurally similar to, but not as massive as those observed in C needles, were detected (Fig. 7m). They were only found in the outer and better illuminated cells and mainly consisted of oxidized pectins (Fig. 7n), without any other histochemically detectable fraction.

Discussion

Visible injury

With 58 ppm h, the CP O_3 exposure was much larger than the 24 ppm h threshold for O_3 injury in C and C + 1 needles as found during fumigation experiments of seedlings (Takemoto et al. 2001). Two types of visible O_3 injury differing according to the needle age were observed in the ponderosa pine needles sampled at CP. In C needles, the light green mottling was typical of O_3 injury with respect to its morphology, distribution and by comparison to O_3 injury documented in *Pinus halepensis*, *strobus* and *uncinata* (Díaz-de-Quijano et al. 2011; Kivimäenpää et al. 2010; Sanz and Calatayud 2012). Mottles found in adjacent C + 1 and older needles showed morphological traits similar to the so-called "winter fleck" injury (brownish dots with sharp edges; Hartmann et al. 2007; Miller and Evans 1974; Stolte 1996), but which were also reminiscent of chlorotic mottling by O_3 stress (symptom frequency increasing with needle age and higher illumination on both abaxial and adaxial needle sides) as found in *Pinus ponderosa* and other conifers (Alvarez et al. 1998a; Flagler and Chappelka 1995; Grulke 2003). With both symptoms adjacent to each other on the same branches, our results suggest that mottling in C and C + 1 needles was related ontologically. In the field; however, mottling is generally observed in C + 1 and older needles (Grulke and Lee 1997; Miller et al. 1997), whereas mottling already occurred in C needles in the examined material. This finding may relate to the higher O_3 exposure in the San Bernardino Mountains than in other O_3-polluted regions of the world (Bytnerowicz et al. 2008).

Microscopic symptoms in C needles

With regard to their distribution and structure, changes typical of O_3 stress were found within mottles and surrounding mesophyll. At the tissue level, the injury gradient, with highest severity in outer mesophyll cell layers next to stomata, together with the unscathed epidermis and vascular bundle were typical of O_3 stress in ponderosa pine

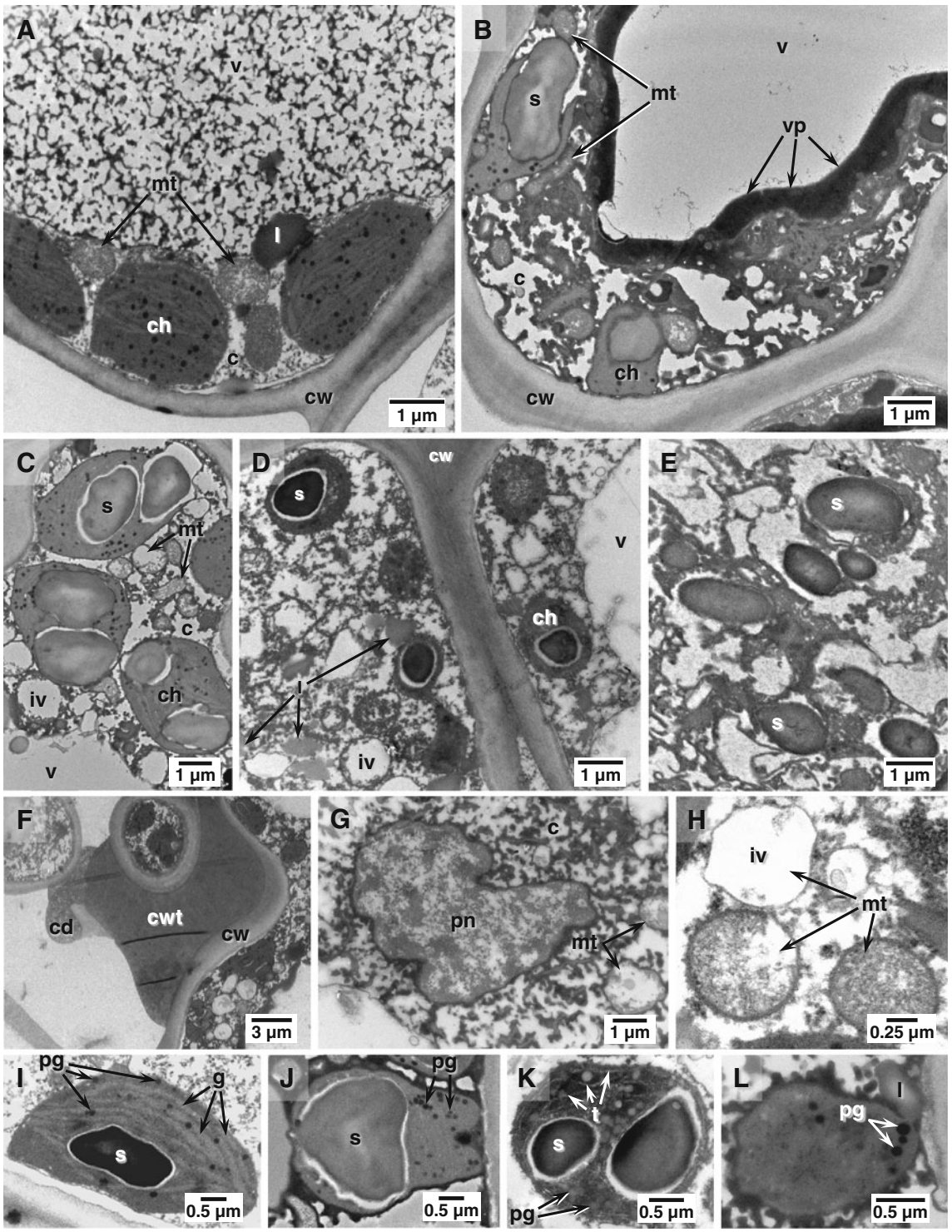

(Evans and Miller 1972a) and other conifers (Alvarez et al. 1998a; Anttonen and Karenlampi 1996; Günthardt-Goerg and Vollenweider 2007; Soda et al. 2000; Sutinen et al. 1990). Symptom proximity to stomata contrasted with the distal location observed in conifer needles (Alvarez et al. 1998a) and leaves from broad-leaved trees (Vollenweider et al. 2003a) with a dorso-ventral polarity. Stomata in foliage of the latter species are primarily located on the shaded abaxial side versus stomata located all around pine needles. Whatever the species, O_3 injury primarily develops within the more light-exposed portions of the mesophyll where it exceeds the cell detoxifying capacities in

◀ **Fig. 6** Ultrastructural changes in cells inside (**b–g**, **j–l**) versus outside (**a**, **h**, **i**) mottling symptoms in mesophyll of C needles showing greenish diffuse mottling. **b** (*mottling*) versus **a** (*no mottling*): The cell structure became increasingly disorganized in cells inside mottles. Notice in **a** the granular structure of proanthocyanidins in the vacuole (*v*). **c–e** With increasing injury, cytoplasm (*c*) condensed in coagulated particles, lipid droplets (*l*) accumulated, the chloroplast (*ch*) and mitochondria (*mt*) structure disrupted and the tonoplast boundary became irregular. In the most degenerated cells, only the starch grains (*s*) could still be recognized. **f** Cell debris (*cd*) and massive cell wall thickening (*cwt*) within the outer mesophyll apoplast. **g** Deformed and highly condensed picnotic nucleus (*pn*). The surrounding cytoplasm particles are condensed and the mitochondria showed advanced degeneration. **h** Degeneration sequence of mitochondria. The matrix and inner membrane system showed injury increasing until only a nearly empty and rather inflated vesicle (*iv*) made of the mitochondria outer membrane was left. **i–j** Degeneration sequence of the chloroplast structure. **i** In cells outside mottles, the stroma appeared condensed and the grana (*g*) poorly resolved. **j–l** Within mottles, the chloroplasts showed a size reduction and an increased plastoglobuli (*pg*) density, further stroma condensation, grana stack and thylakoid (*t*) frequency reduction and poor membrane resolution. In a few cases, the extrusion of lipids (*l*) outside chloroplasts was observed (*L*). Other structures: *cw* cell wall, *vp* vacuolar proanthocyanidins

synergy with photo-oxidative stress (Foyer et al. 1994; Günthardt-Goerg and Vollenweider 2007). Hence, the peculiar injury distribution, with regard to the stomata observed here and in other pines, should relate primarily to the concomitant location of stomata and better illuminated mesophyll cells and secondarily to the proximity to Reactive Oxygen Species (ROS) from O_3-induced oxidative bursts in the apoplast (Baier et al. 2005; Matyssek and Sandermann 2003).

At the cellular level, changes in chloroplasts, especially those in outer cell layers, were characteristic of the effects of O_3 stress (Fink 1999; Holopainen et al. 1996; Kivimäenpää et al. 2005; Soda et al. 2000; Sutinen et al. 1990). Several of these changes, probably contributing to lighter green color in the unshaded needle segments, were also observed in cells outside mottles similar to the findings in O_3 exposed, but asymptomatic foliage (Anttonen and Karenlampi 1996; Kainulainen et al. 2000). Nevertheless, the severity of injury was higher inside than outside mottles and the local disruption process of chloroplasts appears to be the principal reason for the scattered bleached-dot morphology of visible injury. The plastoglobuli accumulation and apparent extrusion into the cytoplasm or vacuoles were indicative of the active involvement of these chloroplastic structures in lipid trafficking and thylakoid membrane turnover, as occurring during senescence and stress events (Bréhélin et al. 2007; Mikkelsen and Heide-Jorgensen 1996; Soda et al. 2000; Tevini and Steinmüller 1985), and of the aforementioned disruption process. Hence, chloroplasts are very sensitive to oxidative stress (Coyne and Bingham 1982; Foyer et al. 1994; Günthardt-Goerg and Vollenweider 2007) as a consequence of the major ROS production occurring in this organelle in comparison to other symplastic sites (Kangasjarvi et al. 2005; Sandermann 1996; Yamasaki et al. 1997). Changes in chloroplast size and plastoglobuli density as a function of chloroplast depth gives further confirmation that O_3 and photo-oxidative stress promote chloroplast injury synergistically.

Among the prominent structural changes, those found in the cell walls of the outer mesophyll cells in mottle centers have never been reported for conifers, but recent observations in *Pinus uncinata* confirm such cell wall modifications as being a response to ozone stress (Díaz-de-Quijano et al. 2011). These massive thickenings were structurally and histochemically similar to characteristic markers of oxidative stress in angiosperms as a consequence of elevated O_3 concentrations (Bâesso Moura et al. 2011; Bussotti et al. 2005; Günthardt-Goerg et al. 1997; Vollenweider et al. 2003a) and other factors causing oxidative stress (Hermle et al. 2007). The detected protein and lignin fraction may be involved in ROS detoxification within the apoplast (Iriti and Faoro 2008; Polle 1997). Within cells from tissue showing mottling symptoms, many structural indications of terminal cell content degeneration and disruption were observed. The missing peroxysomes and degeneration sequence of the mitochondrial membrane and matrix system were particularly indicative of severe oxidative stress inside cells (Jones 2000; Richter 1993; Richter and Schweizer 1997). Besides the amorphous structures, the degradation products included lipid droplets in the cytoplasm and vacuole similar to the findings in Aleppo pines under O_3 stress (Soda et al. 2000) or some broad-leaved species (Mikkelsen and Heide-Jorgensen 1996). All these structural features, together with changes such as the formation of picnotic nuclei or cell content disruption inside restricted groups of mottle cells, meet the structural criteria to identify a hypersensitive-like response reminiscent of that occurring in sensitive broad-leaved trees (Günthardt-Goerg and Vollenweider 2007; Vollenweider et al. 2003a). However, these criteria have been established studying angiosperm species and confirmation from the cell physiology specifically for gymnosperms is still wanting. The occurrence of an accelerated cell senescence response (ACS) in the mesophyll surrounding mottles is suggested by markers such as oxidative injury in chloroplasts and by the accelerated needle shedding (Miller et al. 1997; Takemoto et al. 2001), although O_3-induced and ontological needle aging, presumably because of oxidative stress, differ structurally (Kivimäenpää et al. 2005).

Structural traits in cells outside mottles such as periplasm enlargement, low amounts of starch and perhaps some schloroplast stroma condensation suggest a drought stress effect (Fink 1999) reflecting the environmental

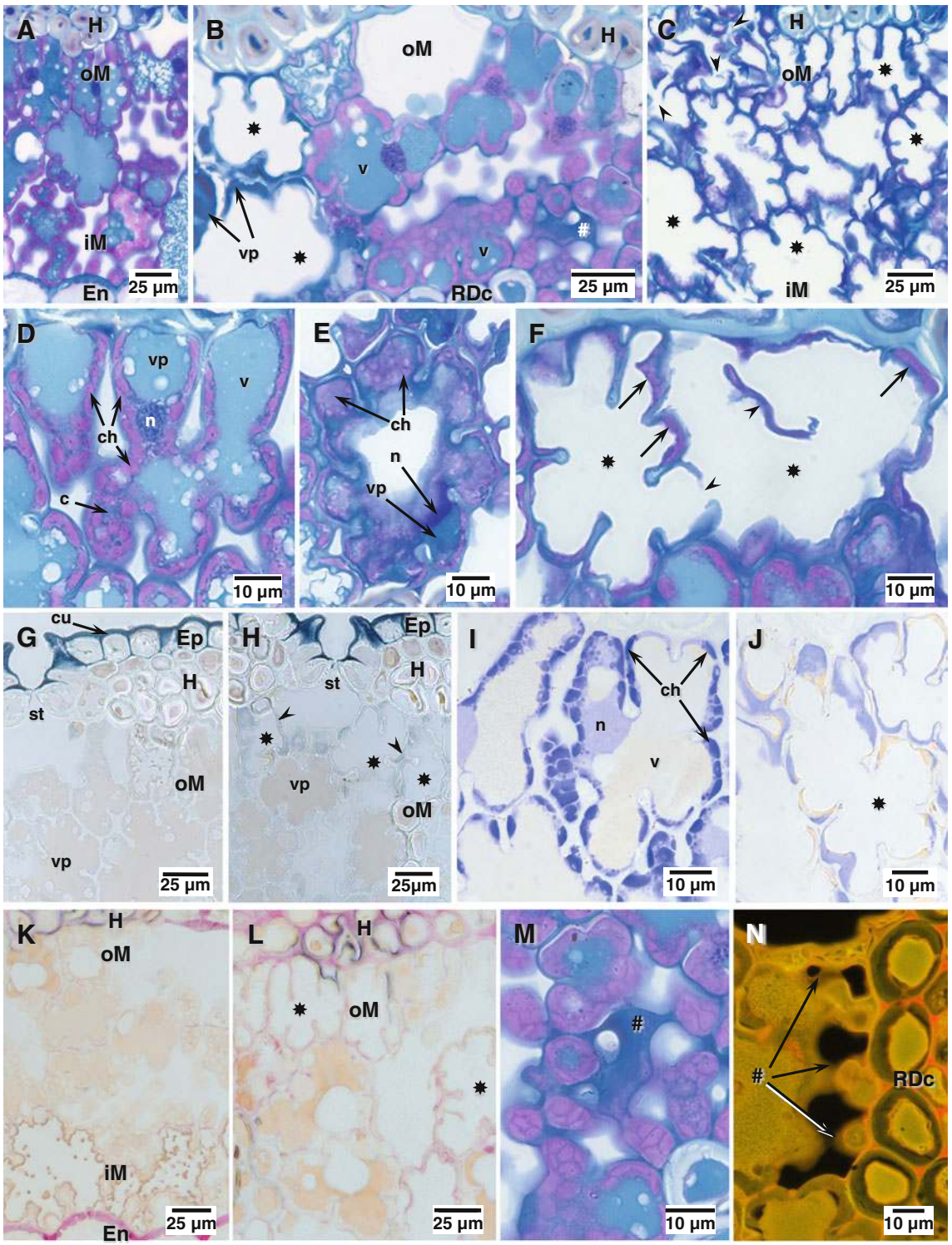

conditions prior to sampling. Inside mottles, the large starch grains together with the low amounts of proanthocyanidins may indicate that the detected hypersensitive-like response occurred early in the vegetation season when still enough soil moisture was available to sustain normal gas exchanges and elevated O_3 uptake (Panek 2004; Panek and Goldstein 2001). Indeed in reference to Seigler (1998), time is needed to accumulate the costly and energy-demanding proanthocyanidins, the deposits of which are generally increased within O_3-symptomatic foliage (Kivimäenpää et al. 2010; Soda et al. 2000; Vollenweider et al. 2003a). At CP, ponderosa pine needles elongate from

◀ **Fig. 7** Structural (**a**–**f**) and histochemical (**g**–**n**) changes at the tissue (**a**–**c**, **k**–**l**) and cellular (**d**–**j**, **m**–**n**) level found inside (**c**, **f**, **h**, **j**, **l**, **m**, **n**) versus outside (**a**, **d**, **g**, **i**, **k**) mottling symptoms and transition zone (**b**, **e**) in mesophyll of C + 1 needles showing brownish mottling. **c**, **f** (Mottling) versus **a**, **d** (no mottling): Cells within chlorotic mottles were dead (*) and cell injury increased from the inner (*iM*) to outer mesophyll layer (*oM*). Cell walls were often broken (*arrowheads*), especially within the outer mesophyll layer, whereas the cell lumen was empty and cell content remnants appressed to cell walls (*arrows*). **b**, **e** (*transition zone*) versus **a**, **d** (*no mottling*): Cells in transition zones showed local thickening of their cell walls (#) and a more or less disrupted cell content. **h** (*Mottling*) versus **g** (*no mottling*): Lipid content increase (*arrowheads*). **j** (*Mottling*) versus **i** (*no mottling*): Protein content decrease. **l** (*Mottling*) versus **k** (*no mottling*): Increased lignification of the cell wall by lignin (*pink*) primarily inlayed in the middle lamella. **m**, **n** Structure and histochemistry of cell wall thickening. Deposits were amorphous and consisted mostly of pectin as shown by their reactivity with coriphosphine. In comparison to the pectin-specific *orange color*, as found in the cell walls of nearby resin duct sheath cells (RDc), the *brownish color* of thickenings (#→) indicated an increased oxidation. Other structures: *c* cytoplasm, *ch* chloroplasts, *En* endodermis, *Ep* epidermis, *H* hypodermis, *n* nucleus, *st* stomata, *v* vacuole, *vp* vacuolar proanthocyanidins

April/May until the end of July during dry years (Grulke et al. 1998); In 2006, this was the period during which the highest O_3 concentrations were measured.

Microscopic symptoms in C + 1 needles

Structural injury underlying chlorotic mottling in C + 1 needles also showed typical indications of O_3 stress with regard to its distribution and markers of oxidative stress in apoplast and symplast. Hence, it showed the same injury pattern as found in C needles which also suggests a hypersensitive-like plant response. The necrotic cell structure and distribution was similar to that reported for C + 1 and older needles of *Abies religiosa* (Alvarez et al. 1998a) or *P. halepensis* (Kivimäenpää et al. 2010). In comparison to C needles however, several structural traits were observed only in older foliage: (1) large injuries encompassing several stomata lines, (2) broken cells, (3) less developed cell wall thickenings and (4) more disrupted and oxidized cell structures. Hence, disruptive processes in symptomatic tissues were more advanced in C + 1 than C needles which might relate to the larger time lapse since mottling establishment, as suggested by the larger amounts of proanthocyanidins in surrounding and still living versus dead mottle cells. However, the rupture and removal of entire cells were clearly not an O_3 effect and suggests mechanical injury by another abiotic stress factor, presumably frost (Fink 1999). The outer mesophyll location of this injury is also indicative of the aforementioned stress factor. Other indications of winter fleck injury such as symptoms in inner mesophyll and vascular bundles (Fink 1999; Miller and Evans 1974) were generally missing. In synthesis, these observations suggest an injury initially caused by O_3 then aggravated during winter, presumably following the formation of ice crystals at the most damaged locations (Fink 1999). The injury was likely further intensified during the next growing season as a consequence of steady oxidative stress at the periphery of the symptomatic area. Hence, interaction between O_3 and frost stress is suggested by these structural changes—a process which, with the contribution of supplementary biotic and abiotic stress factors, could cause a frost hardiness reduction in the affected foliage (Fink 1999).

Conclusion

In conclusion, structural injury found in the apoplast and symplast of mesophyll cells underlying the mottling symptoms in ponderosa pine needles contrasted with those in surrounding areas and were indicative of severe oxidative stress suggesting hypersensitive-like responses to O_3, as described in angiosperms. Other environmental stressors, i.e. drought in C and frost in C + 1 needles, contributed sizably to the morphological singularities of the symptomatic areas. Hence, structural injury underlying mottling was not only useful to gain insights about important effects of ozone on cell physiology, but also to better ascertain the diagnosis in a context of high air pollution, such as in southern California, and to distinguish the effects of other concomitant stress factors.

Acknowledgments The authors gratefully acknowledge the technical support of Susan Schilling for the air pollution data calculation and mapping, of Lara Pfister for light microscopy and of the Center for Microscopy and Image Analysis of the University of Zürich for electron microscopy.

References

Alvarez D, Laguna G, Rosas I (1998a) Macroscopic and microscopic symptoms in *Abies religiosa* exposed to ozone in a forest near Mexico City. Environ Pollut 103:251–259

Alvarez ME, Pennell RI, Meijer PJ, Ishikawa A, Dixon RA, Lamb C (1998b) Reactive oxygen intermediates mediate a systemic signal network in the establishment of plant immunity. Cell 92:773–784

Anttonen S, Karenlampi L (1996) Slightly elevated ozone exposure causes cell structural changes in needles and roots of Scots pine. Trees 10:207–217

Anttonen S, Herranen J, Peura P, Karenlampi L (1995) Fatty-acids and ultrastructure of ozone-exposed Aleppo pine (*Pinus halepensis* Mill) needles. Environ Pollut 87:235–242

Anttonen S, Sutinen ML, Heagle AS (1996) Ultrastructure and some plasma membrane characteristics of ozone-exposed loblolly pine needles. Physiol Plant 98:309–319

Arbaugh MJ, Miller PR, Carroll JJ, Takemoto B, Procter T (1998) Relationships of ozone exposure to pine injury in the Sierra Nevada and San Bernardino Mountains of California, USA. Environ Pollut 101:291–301

Arkley RJ (1981) Soil moisture use by mixed conifer forest in a summer-dry climate. Soil Sci Soc Am J 45:423–427

Bâesso Moura B, Ribeiro de Souza S, Segala Alves E (2011) Structural responses of *Ipomea nil* (L.) Roth 'Scarlet O'Hara' (Convolvulaceae) exposed to ozone. Acta Bot Brasilica 25:122–129

Baier M, Kandlbinder A, Golldack D, Dietz KJ (2005) Oxidative stress and ozone: perception, signalling and response. Plant Cell Environ 28:1012–1020

Bréhélin C, Kessler F, van Wijk KJ (2007) Plastoglobules: versatile lipoprotein particles in plastids. Trends Plant Sci 12:260–266

Brundrett MC, Kendrick B, Peterson CA (1991) Efficient lipid staining in plant material with sudan red 7B or fluoral yellow 088 in polyethylene glycol-glycerol. Biotech Histochem 66:111–116

Bussotti F, Agati G, Desotgiu R, Matteini P, Tani C (2005) Ozone foliar symptoms in woody plant species assessed with ultrastructural and fluorescence analysis. New Phytol 166:941–955

Bytnerowicz A, Fenn ME (1996) Nitrogen deposition in California forests: a review. Environ Pollut 92:127–146

Bytnerowicz A, Arbaugh A, Schilling S, Fraczek W, Alexander D, Dawson P (2007) Air pollution distribution patterns in the San Bernardino Mountains of southern California: a 40-year perspective. Sci World J 7:98–109

Bytnerowicz A, Arbaugh M, Schilling S, Fraczek W, Alexander D (2008) Ozone distribution and phytotoxic potential in mixed conifer forests of the San Bernardino Mountains, Southern California. Environ Pollut 155:398–408

Clark G (1981) Staining procedures, 4th edn. Williams & Wilkins, Baltimore

Coyne PI, Bingham GE (1982) Variation in photosynthesis and stomatal conductance in an ozone-stressed ponderosa pine stand—light response. For Sci 28:257–273

Dalstein L, Vas N (2005) Ozone concentrations and ozone-induced symptoms on coastal and alpine Mediterranean pines in southern France. Water Air Soil Pollut 160:181–195

Davis DD (1977) Response of ponderosa pine primary needles to separate and simultaneous ozone and PAN exposure. Plant Dis Rep 61:640–644

de Bauer MD, Hernandez-Tejeda T (2007) A review of ozone-induced effects on the forests of central Mexico. Environ Pollut 147:446–453

Diaz-de-Quijano M, Penuelas J, Ribas A (2009) Increasing interannual and altitudinal ozone mixing ratios in the Catalan Pyrenees. Atmos Environ 43:6049–6057

Díaz-de-Quijano M, Peñuelas J, Menard T, Vollenweider P (2011) Visible and microscopical ozone injury in mountain pine (*Pinus mugo* subsp. uncinata) foliage from the Catalan Pyrenees. International Conference Ozone, climate change and forests, 14–16 June 2011, Prague, Czech Republic. http://cost-fp0903.ipp.cnr.it/Downloads/Prague/BookAbstracts.pdf. Accessed 11 June 2012

Evans LS, Fitzgerald GA (1993) Histological effects of ozone on slash pine (*Pinus elliotti* var. densa). Environ Exp Bot 33:505–513

Evans LS, Leonard MR (1991) Histological determination of ozone injury symptoms of primary needles of giant sequoia (*Sequoiadendron giganteum* Bucch). New Phytol 117:557–564

Evans LS, Miller PR (1972a) Comparative needle anatomy and relative ozone sensitivity of four pine species. Can J Bot 50:1067–1071

Evans LS, Miller PR (1972b) Ozone damage to ponderosa pine—histological and histochemical appraisal. Am J Bot 59:297–304

Feder N, O'Brien TP (1968) Plant microtechnique: some principles and new methods. Am J Bot 55:123–142

Fenn ME, Jovan S, Yuan F, Geiser L, Meixner T, Gimeno BS (2008) Empirical and simulated critical loads for nitrogen deposition in California mixed conifer forests. Environ Pollut 155:492–511

Fink S (1999) Pathological and regenerative plant anatomy. Encyclopedia of plant anatomy, vol XIV/6. Gebrüder Bornträger, Berlin, Stuttgart

Flagler RB, Chappelka AH (1995) Growth response of southern pines to acidic precipitation and ozone. In: Fox S, Mickler RA (eds) Impact of air pollutants on southern pine forest. Ecological Studies 118. Springer, Berlin, pp 388–424

Foyer CH, Lelandais M, Kunert KJ (1994) Photooxidative stress in plants. Physiol Plant 92:696–717

Gahan PB (1984) Plant histochemistry and cytochemistry. Academic Press, London

Gerlach D (1984) Botanische Mikrotechnik, 3rd edn. Thieme Verlag, Stuttgart

Grulke NE (2003) The physiological basis of O_3 injury assessment attributes in Sierran conifers. In: Bytnerowicz A, Arbaugh M, Alonso R (eds) Assessment of O_3 distribution and its effects on Sierra Nevada ecosystems. Developments in Environmental Science 2. Elsevier, The Hague, pp 55–81

Grulke NE, Balduman L (1999) Deciduous conifers: high N deposition and O-3 exposure effects on growth and biomass allocation in ponderosa pine. Water Air Soil Pollut 116:235–248

Grulke NE, Lee EH (1997) Assessing visible ozone-induced foliar injury in ponderosa pine. Can J For Res 27:1658–1668

Grulke NE, Andersen CP, Fenn ME, Miller PR (1998) Ozone exposure and nitrogen deposition lowers root biomass of ponderosa pine in the San Bernardino Mountains, California. Environ Pollut 103:63–73

Grulke NE, Minnich RA, Paine TD, Seybold SJ, Chavez DJ, Fenn ME, Riggan PJ, Dunn A (2009) Air pollution increases forest susceptibility to wildfires: a case study in the San Bernardino Mountains in southern California. In: Bytnerowicz A, Arbaugh MJ, Riebau AR, Andersen C (eds) Wildland fires and air pollution. Developments in Environmental Science, vol 8. Elsevier, Amsterdam, pp 365–403

Günthardt-Goerg MS, Vollenweider P (2007) Linking stress with macroscopic and microscopic leaf response in trees: new diagnostic perspectives. Environ Pollut 147:88–467

Günthardt-Goerg MS, McQuattie CJ, Scheidegger C, Rhiner C, Matyssek R (1997) Ozone-induced cytochemical and ultrastructural changes in leaf mesophyll cell walls. Can J For Res 27:453–463

Hartmann G, Nienhaus F, Butin H (2007) Farbatlas Waldschäden. 3. Auflage. Diagnose von Baumkrankheiten. 3. Auflage. Eugen Ulmer KG, Stuttgart

Hermle S, Vollenweider P, McQuattie CJ, Matyssek R, Günthardt-Goerg MS (2007) Leaf responsiveness of field-grown *Populus tremula* and *Salix viminalis* to soil contamination by heavy metals and rainwater acidity. Tree Physiol 27:1517–1531

Holopainen T, Anttonen S, Palomaki V, Kainulainen P, Holopainen JK (1996) Needle ultrastructure and starch content in Scots pine and Norway spruce after ozone fumigation. Can J Bot 74:67–76

Iriti M, Faoro F (2008) Oxidative stress, the paradigm of ozone toxicity in plants and animals. Water Air Soil Pollut 187:285–301

Jones A (2000) Does the plant mitochondrion integrate cellular stress and regulate programmed cell death? Trends Plant Sci 5:225–230

Kainulainen P, Utriainen J, Holopainen JK, Oksanen J, Holopainen T (2000) Influence of elevated ozone and limited nitrogen availability on conifer seedlings in an open-air fumigation system: effects on growth, nutrient content, mycorrhiza, needle ultrastructure, starch and secondary compounds. Glob Change Biol 6:345–355

Kangasjarvi J, Jaspers P, Kollist H (2005) Signalling and cell death in ozone-exposed plants. Plant Cell Environ 28:1021–1036

Karnosky DF, Skelly JM, Percy KE, Chappelka AH (2007) Perspectives regarding 50 years of research on effects of tropospheric ozone air pollution on US forests. Environ Pollut 147:489–506

Kivimäenpää M, Sellden G, Sutinen S (2005) Ozone-induced changes in the chloroplast structure of conifer needles, and their use in ozone diagnostics. Environ Pollut 137:466–475

Kivimäenpää M, Sutinen S, Calatayud V, Sanz MJ (2010) Visible and microscopic needle alterations of mature Aleppo pine (*Pinus halepensis*) trees growing on an ozone gradient in eastern Spain. Tree Physiol 30:541–554

Levine A, Pennell RI, Alvarez ME, Palmer R, Lamb C (1996) Calcium-mediated apoptosis in a plant hypersensitive disease resistance response. Curr Biol 6:427–437

Matyssek R, Sandermann H (2003) Impact of ozone on trees: an ecophysiological perspective. Progress in Botany 64. Springer, Heidelberg, pp 349–404

McQuattie CJ, Schier GA (1993) Effect of ozone and aluminium on pitch pine (*Pinus rigida*) seedlings—needle ultrastructure. Can J For Res 23:1375–1387

Mikkelsen TN, Heide-Jorgensen HS (1996) Acceleration of leaf senescence in *Fagus sylvatica* L. by low levels of tropospheric ozone demonstrated by leaf colour, chlorophyll fluorescence and chloroplast ultrastructure. Trees 10:145–156

Miller PR, Evans LS (1974) Histopathology of oxidant injury and winter fleck injury on needles of western pines. Phytopathology 64:801–806

Miller PR, McBride JR (1999) Oxidant air pollution impacts in the montane forests of Southern California. Ecol Studies, vol 134. Springer, New York

Miller PR, Rechel J (1999) Temporal changes in crown condition indices, needle litterfall, and collateral needle injuries of ponderosa and Jeffrey pines. In: Miller PR, McBride JR (eds) Oxidant air pollution impacts in the montane forests of southern California: a case study of the San Bernardino Mountains. Ecol Stud 134. Springer, New York, pp 164–178

Miller PR, Taylor OC, Parmeter JR, Cardiff EA (1963) Ozone injury to foliage of *Pinus ponderosa*. Phytopathology 53:1072–1076

Miller PR, Arbaugh MJ, Temple PJ (1997) Ozone and its known and potential effects on forests in Western United States. In: Sandermann H Jr, Wellburn AR, Heath RL (eds) Forest decline and ozone. Ecol Stud 127. Springer, Berlin, pp 39–67

Munck L (1989) Fluorescence analysis in food. Longman Scientific and Technical, Harlow

Padgett PE, Parry SD, Bytnerowicz A, Heath RL (2009) Image analysis of epicuticular damage to foliage caused by dry deposition of the air pollutant nitric acid. J Environ Monit 11:63–74

Panek JA (2004) Ozone uptake, water loss and carbon exchange dynamics in annually drought-stressed *Pinus ponderosa* forests: measured trends and parameters for uptake modeling. Tree Physiol 24:277–290

Panek JA, Goldstein AH (2001) Response of stomatal conductance to drought in ponderosa pine: implications for carbon and ozone uptake. Tree Physiol 21:337–344

Polle A (1997) Defense against photooxidative damage in plants. In: Scandalios JG (ed) Oxidative stress and the molecular biology of antioxidant defenses. Cold Spring Harbor Laboratory Press, New York, pp 623–666

Richards BL Sr, Taylor OC, Edmunds GF Jr (1968) Ozone needle mottle of pine in southern California. J Air Pollut Control Assoc 18:73–77

Richter G (1993) Métabolisme des végétaux. Physiologie et Biochimie. Presses polytechniques et universitaires romandes, Lausanne

Richter Ch, Schweizer M (1997) Oxidative stress in mitochondria. In: Scandalios JG (ed) Oxidative stress and the molecular biology of antioxidant defenses. Cold Spring Harbor Laboratory Press, New York, pp 169–200

Sandermann H (1996) Ozone and plant health. Annu Rev Phytopathol 34:347–366

Sanz MJ, Calatayud V (2012) Ozone injury in European forest species. http://www.ozoneinjury.org. Accessed 11 June 2012

Sarkar SK, Howarth RE (1976) Specificity of the vanilin test for flavonoids. J Agric Food Chem 24:317–320

Seigler DS (1998) Plant secondary metabolism. Kluwer Academic Publishers, Boston

Soda C, Bussotti F, Grossoni P, Barnes J, Mori B, Tani C (2000) Impacts of urban levels of ozone on *Pinus halepensis* foliage. Environ Exp Bot 44:69–82

Stolte K (1996) Symptomology of ozone injury to pine foliage. In: Miller P, Stolte K, Duriscoe D (eds) General Technical Report PSW-GTR-155-Web. http://www.fs.fed.us/psw/publications/documents/gtr-155/publisher.html. Accessed 11 June 2012

Sutinen S (1986) Ultrastructure of mesophyll-cells in and near necrotic spots on otherwise green needles of Norway spruce. Eur J For Pathol 16:379–384

Sutinen S, Skarby L, Wallin G, Sellden G (1990) Long-term exposure of Norway spruce, *Picea-Abies* (L) Karst, to ozone in open-top chambers. 2. Effects on the ultrastructure of needles. New Phytol 115:345–355

Takemoto BK, Bytnerowicz A, Fenn ME (2001) Current and future effects of ozone and atmospheric nitrogen deposition on California's mixed conifer forests. For Ecol Manage 144:159–173

Tevini M, Steinmüller D (1985) Composition and function of plastoglobuli. Planta 163:91–96

Utriainen J, Holopainen T (1998) Ultrastructural and growth responses of young Scots pine seedlings (*Pinus sylvestris*) to increasing carbon dioxide and ozone concentrations. Chemosphere 36:795–800

Vollenweider P, Günthardt-Goerg MS (2006) Diagnosis of abiotic and biotic stress factors using the visible symptoms in foliage. Environ Pollut 140:562–571

Vollenweider P, Ottiger M, Günthardt-Goerg MS (2003a) Validation of leaf ozone symptoms in natural vegetation using microscopical methods. Environ Pollut 124:101–118

Vollenweider P, Woodkock H, Kelty MJ, Hofer R-M (2003b) Reduction of stem growth and site dependency of leaf injury in Massachusetts black cherries exhibiting ozone symptoms. Environ Pollut 125:467–480

Walter H, Lieth H (1967) Klimadiagram-Weltatlas. VEB Gustav Fischer Verlag, Jena

Weis KG, Polito VS, Labavitch JM (1988) Microfluorometry of pectic materials in the dehiscence zone of almond (*Prunus dulcis* [Mill] DA Webb) fruits. J Histochem Cytochem 36:41–1037

Wetzel S, Demmers C, Greenwood JS (1989) Spherical organelles, analogous to seed protein bodies, fluctuate seasonally in parenchymatous cells of hardwoods. Can J Bot 67:3439–3445

Yamasaki H, Sakihama Y, Ikehara N (1997) Flavonoid-peroxidase reaction as a detoxification mechanism of plant cells against H_2O_2. Plant Physiol 115:1405–1412